

# Numerical Simulation of 3D Reacting Flow in Gas Turbine Combustors. Part II: Detailed Results.

S. DURANTI, S. TRAVERSO, F. PITTALUGA

DIMSET, Department of Fluid Machines, Energy Systems and Transportation  
University of Genova, via Montallegro 1, 16145 Genova - Italy

**ABSTRACT:** The present Part II of the paper deals with the application of NastComb, a 3D time-dependent turbulent reactive-flow Navier-Stokes solver, toward the performance prediction of the (annular) combustor of the Ansaldo-Siemens V64.3A heavy-duty gas turbine. Whilst the main features of the solver are presented in Part I of the paper, detailed results of the relevant fluid-dynamical and thermo-chemical variables are here shown with particular attention given to an important validation of the solver, in terms of wall temperature distributions' numerical/experimental comparison. In addition, emissive (NO<sub>x</sub>) predictions are given, together with a first tentative assessment of the overall combustor thermo-acoustical stability, investigated by following its dynamical response after an induced pressure perturbation.

## INTRODUCTION

Whilst Part I of the study (same Ref. of this Part II) deals with the analytical/numerical structure of the 3D turbulent reactive-flow Navier-Stokes solver named NastComb<sup>1,2</sup>, mainly developed by the authors, this Part II will show detailed results of its application to the (annular) combustor of the Ansaldo-Siemens V64.3A gas-turbine.

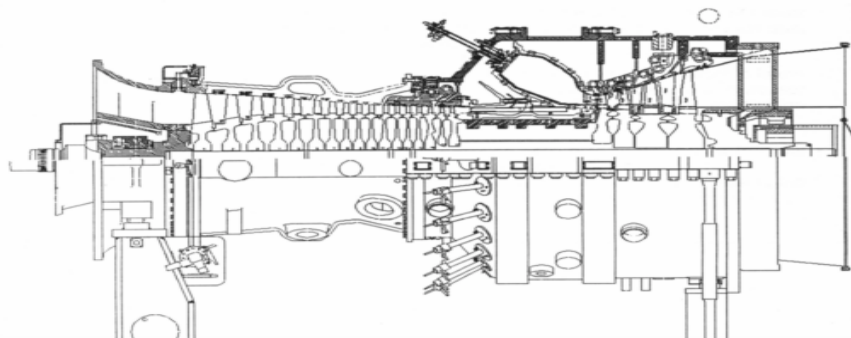
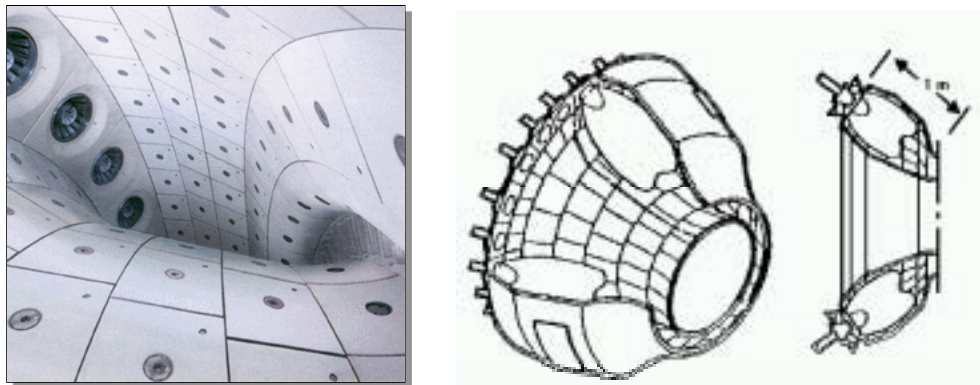


Fig.1 – The Ansaldo-Siemens V64.3A gas turbine

This machine (fig.1) is a single-axis, 70 MW-class, heavy-duty, dry low-NO<sub>x</sub> gas-turbine with annular combustor (16 bar, 24 premix hybrid burners), capable to burn both gas- and liquid-fuels.

As sketched in Fig.2, the annular combustor is equipped with 24 burners and its walls are fully covered with heavy, contoured, inconel tiles, provided with many holes and interstices for a properly distributed admission of cooling air. Anyhow, and by far, the main air admission is through the burners, as primary/secondary combustion air. The burner (Fig.3) is “hybrid”, for it can operate, both for gas and liquid fuels, either in premixed- or diffusion-flame modalities. As well known, the latter produce higher NO<sub>x</sub> levels, due to higher primary-zone temperatures, but also more stable flames. In Table 1 (below), typical CO and NO<sub>x</sub> emission levels are shown for the premixed-flame modalities, respectively for gas and liquid fuel operation.



**Fig. 2 - Ansaldo-Siemens V64.3A annular combustor**

NO <sub>x</sub> control mode	-	gas premix		oil premix	
		dry	wet	dry	wet
Emissions: NO <sub>x</sub>	ppmv	35	25	100	50
Emissions: CO	ppmv	10	10	10	10
Unburnt hydrocarbons	ppmv	4	4	6	6

**Table 1 - Burner's emissions in premixed-flame modalities**

In line with a well established tradition of research collaboration between Ansaldo Turbine Dept. and DIMSET, the authors pursued the ambitious target of supporting, from a theoretical/numerical (academic) perspective, the final phases of the V64.3A annular combustor (industrial) project as well as the optimised assessment of its operational parameters, both in terms of emissions and stability. To this end, advantage was taken from a parallel, unique opportunity: namely, the progressive availability of detailed experimental data coming from the Siemens/KWU full-size, full-power, gas-turbine test stand in Berlin, where an actual V64.3A machine was undergoing a thorough performance-testing campaign,

both as a whole unit and in its components. Whilst many sets of data cannot be presented and discussed for reasons of industrial confidentiality, for some, the manufacturer has allowed publication. Among these latter, a few are here utilised for validating the theoretical predictions that are now following.

### NUMERICAL PREDICTIONS

The numerical predictions of the overall turbulent reactive flow-field inside the V64.3A combustor started with a first (unreactive) simulation of the single-burner flow-field, necessary to compute the burner-outlet velocities to be utilised as combustor-inlet velocity boundary conditions. In this sense, a sort of two-components (burner and combustor) numerical interaction was adopted, which turned out quite useful in terms of overall numerical efficiency. Fig.4 shows the structured numerical mesh of the annular combustor, made up of 44,500 cells, representing a 15° sector (1/24 of the whole annular geometry), with the burner exhaust localized at the bottom. The mesh is multiblock-type: in this way one can easily refine locally the grid-cell texture where gradients are steep or the solution is required to be particularly accurate.

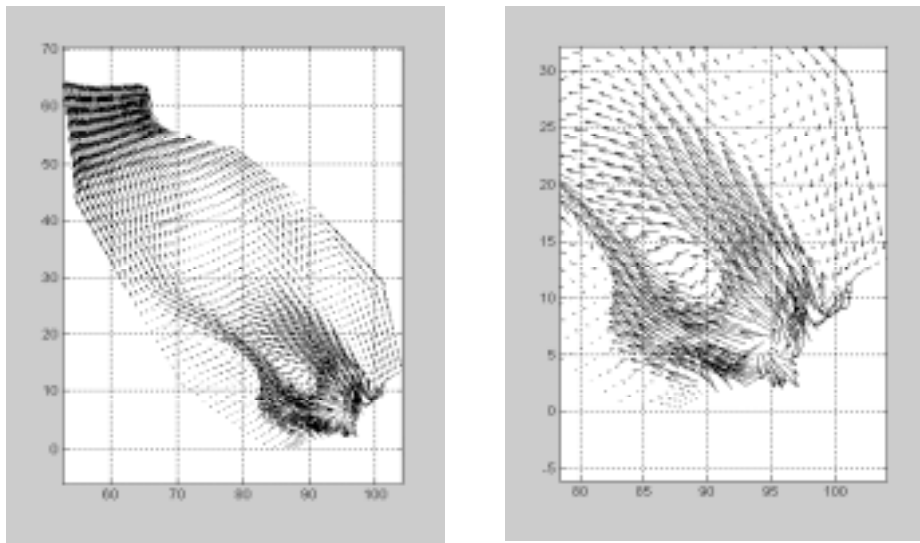
Velocity boundary conditions have been derived from the burner cold-simulation and compared with LDV laboratory results<sup>2</sup>. The burner entails an axial and a diagonal swirler, with nominal respective air flow rates of 0.46 and 4.75 kg/s. The natural-gas fuel, lean premixed within the latter swirler, has a flow rate of 0.147 kg/s. A diffusion pilot-flame is fed with additional 0.011 kg/s of fuel. Air and fuel inlet temperatures were set to 682 K, at the nominal operating pressure of 16 bar. Not in contradiction with manufacturer's indications, and mainly for simplifying the heavy computations, nearly-adiabatic wall boundary-conditions were imposed, entailing with this the net result of all heat transfer modalities, inclusive of radiation. Ceramic wall-tiles emissivity is set to 0.7 and burnt gases emissivity is computed from the concentrations of H<sub>2</sub>O and CO<sub>2</sub> species.



**Fig. 3 - The V643.A burner**

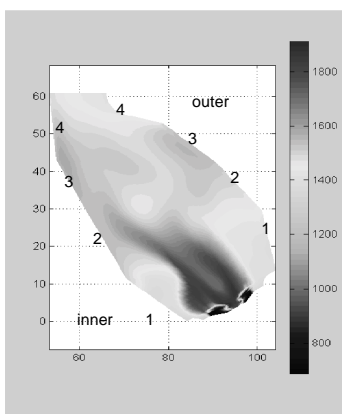


**Fig.4 - Combustor computational mesh**

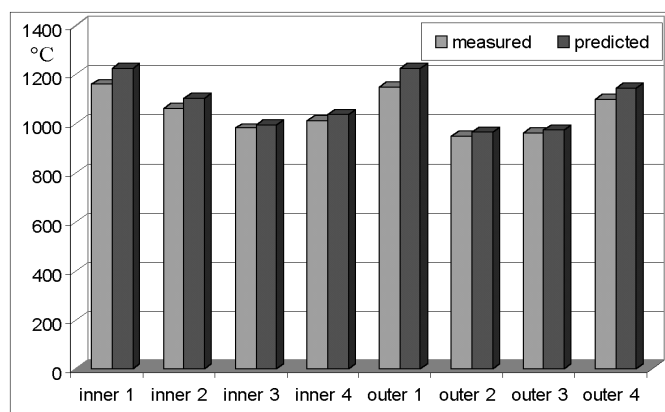


**Fig. 5 - Velocity field in the meridional plane and detail at combustor inlet**

Fig.5 shows the reactive-situation velocity field in a combustor meridional plane passing through the symmetry axis of the burner. Note the complex flow field, with the presence of several, large recirculating zones, as induced by the three-dimensional interactions of the many swirlers among themselves, with the annular geometry and with the combustion process. It seems as if the overall combustor length, which appears very compact (also in view of lowering hot gasses' residence times for controlling NO<sub>x</sub>), would be selected of the shortest dimension compatible with a re-organised, recirculation-free, outlet flow-field. To this aim, a strong contribution is obviously given by the contraction of the meridional contour toward the exit section, with the corresponding local re-acceleration of the flow: notice that this flow-reorganisation process is quite successful, with a rather uniform meridional velocity profile at the outlet section, to the advantage of the operation of the power turbine.



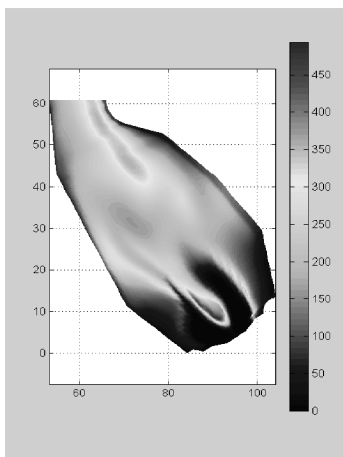
**Fig. 6 - Temperature field**



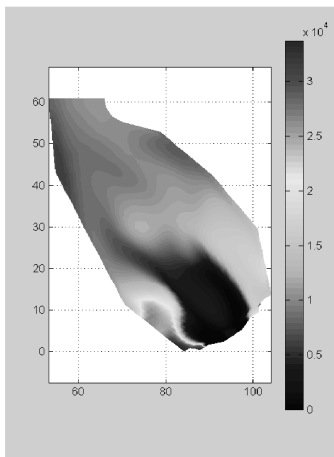
**Fig. 7 – Wall-temperature distributions comparisons**

Fig.6 presents the temperature field in the meridian plane. Similarly to what just discussed in connection with the flow-field behaviour, notice the progressive smoothing of the temperature differences as the outlet zone of the combustor is approached. In this respect, an additional observation turns out absolutely fundamental, and motivating this combustor design: apart from the localised zone where the diffusion pilot-flame is situated, and thus in line with the lean, premixed-flame modality here assumed and investigated, the said temperature differences, together with their absolute levels, appear anyhow limited even in primary zones, to the advantage of emissions control (Dry Low NOx). Particularly along the combustor walls notice the absence of any localised temperature overshoot, a further, important observation in terms of combustor operational safety.

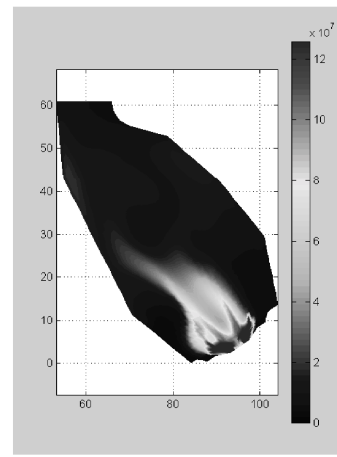
In the same Fig.6, the (meridian-section) locations are indicated, with numbers, where wall-temperature measurements were taken on the Siemens gas-turbine test-stand in Berlin. Following what discussed in Part I of this paper, and applying the radiative/convective thermal boundary conditions under a nearly-adiabatic assumption, NastComb's predictions of the meridian-plane distributions of wall temperatures are given in Fig.7 together with the corresponding experimental measurements. "Inner" and "outer" refer to wall meridian-profiles at shorter and, respectively, longer distances from the machine axis. It can be seen that the temperature trends are almost everywhere well captured, symptom that both the overall combustion process and the radiation field predictions (with the related wall-tiles' radiation shape-factors and emissivities) are correct. The almost general, although limited, overprediction of wall temperatures may be related to the adiabatic-wall assumption, which forces higher tile-temperatures in order to emit back an amount of heat which actually is transferred through the walls.



**Fig. 8 - Turb. kin. en. ( $\text{m}^2/\text{s}^2$ )**



**Fig.9 - NO density ( $\text{g}/\text{cm}^3$ )**



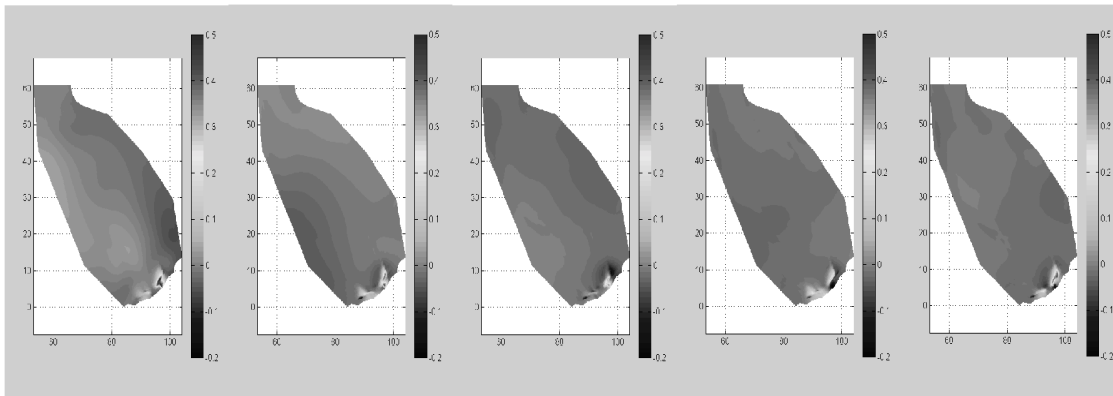
**Fig.10 - OH density ( $\text{g}/\text{cm}^3$ )**

Fig.8 shows the levels of turbulent kinetic energy, which are in line with what already observed in connection with the velocity field. Interesting is to watch, in the very primary zone, the combined effects of the combustion heat release and of the swirling flow toward a sharp decrease of turbulent energy, a well known, but perhaps also anti-intuitive outcome. This is one more reason for saying a word of caution when fluid-dynamical experimental

evidence, even drawn from full-scale but unreactive laboratory measurements, is transferred and applied to real combustor analysis. Whilst the turbulent energy appears to increase in the boundary layers along the walls, its clear trend for the core-flow is toward a smooth distribution well ahead of the outlet section. Though not directly shown by Fig.8 (which is in absolute values of the turbulent energy), the final acceleration of the flow is seen to induce a strong decrease in turbulent intensity (in percent).

Figs.9 and 10 present respectively the NO and OH densities. For a better interpretation of these figures, it is useful to correlate them to the temperature behaviour (Fig.6) which shows a maximum in the nearness of the diffusion pilot-flame (lower-left of the meridian section), where fuel concentration is higher and premixing is not induced. According to theory, where temperature is high, NO and OH concentrations sharply increase, as attested by above figures. However, in this connection, an additional information turns out important, which can be drawn from the fluid dynamical picture given in Fig.5. Exactly the zone where the pilot flame is localised shows a low-velocity recirculation pattern, that for sure is imposing high residence times for the hot gasses, in this way further increasing the kinetic production of thermal NOx . It should be interesting to check how the emissions picture would change as a result of displacing the pilot flame toward a recirculation-free location: an analysis of this kind is already under way, by means of a parametric application of NastComb in correspondence of different pilot flame positions and orientations.

Finally, Fig.9 presents a first tentative effort toward the assessment of the thermo-acoustical stability characteristics of the overall combustion system. Indeed, for a combustor design like the present one, expressly conceived to operate in very-lean, fully-premixed regimes with highly smooth axial/azimuthal distributions of the thermo-fluid-dynamical parameters (temperature, species densities, turbulent energy), this sort of information is absolutely vital, even from an overall machine's safety point-of-view. To investigate numerically the transient response, to thermo-acoustic waves, of the combustor in its meridian plane, a sudden pressure perturbation has been imposed artificially on to all the combustor cells after the steady-state was reached, in fully reactive conditions. Namely, a 10% step variation, with respect to local cell pressure, has been imposed through a Dirac-like pressure-impulse, say at  $t = t_0$ . Then, the process is monitored at  $t = t_0 + 1.30e-4$  s,  $t = t_0 + 3.89e-4$  s,  $t = t_0 + 6.48e-4$  s,  $t = t_0 + 7.77e-4$  s,  $t = t_0 + 1.3e-3$  s. In Fig.11, the behavior of the waves appears as following a process characterized by well defined frequencies, at least in the meridian direction: their order of magnitude is not dissimilar from the experimental evidence (Berlin test-stand measurements, subject to confidentiality). The study is now under way to better correlate this sort of information with both the operational and the design parameters of the combustion system: the aim is, first, that of correctly interpreting the complex phenomenon, then, also that of trying to set up a strategy suitable to progressively extend the stability range of the combustor.



**Fig.11 - Time-dependent thermo-acoustic waves behavior**

## CONCLUSIONS

The authors feel to have developed, and presented in this paper (Part I and II), an advanced numerical tool for combustion processes' prediction that, at least in perspective, can become a valid competitor with the widespread offer of commercial codes in the field. Intrinsic, almost unique, features of NastComb are a fully time-dependent lagrangian-eulerian scheme, a higher-order, scale-interacting, variable-density turbulence model, a quasi-global thermo-chemical scheme that, extended with mixing-controlled Arrhenius kinetics, implements a proper set of elementary reactions to capture both the main and trace species evolution.

The still-today highly complex task of reliably predicting combustion processes typical of gas turbine combustors has been approached, anywhere possible, more with "simulative" strategies than "modeling" procedures: this point is exactly reflected in the just-above listed characteristics of the code, and in the choice of not resorting to any PDF-based criterion to "model" combustion. Motivation for all this can also be found in the long-term objective of keeping a code's structure suitable to automatically, and physically, respond to large-scale vortex dynamics any time a fine-enough grid can be utilised. The first step toward this goal has been here already presented, namely the fast, time-dependent analysis of the thermo-acoustical waves behaviour, which appear captured in a rather efficient way. From a more application-oriented point of view, the experimental validation of NastComb predictions, with regard to wall-temperature distributions, is considered as an important result for further enhancing the code reliability.

Finally, the important R&D connection recently established, in the technological sector of advanced gas turbine plants, between Ansaldo Turbine Dept. and DIMSET, should prompt also a side-outcome, which is not a secondary one: namely, that of progressively field-validating a series of numerical tools such as NastComb so to succeed in "commissioning" to these tools really incisive and qualifying actual-design tasks.

## REFERENCES

1. Pittaluga, F.; Luccoli, R.; Traverso, S.: "Improvement of Numerical Predictions of Methane Turbulent Diffusion Flames By Considering Radiation Effects"; 27<sup>th</sup> Int. Symposium on Combustion, The Combustion Institute, Proceedings, Boulder, Co., Aug.1998
2. Traverso, S.: "Previsione time-dependent del flusso 3D combustivo in combustore per turbina a gas"; PhD Thesis, University of Genova, Italy, February 2000